

## Evaluation of microstructure and mechanical properties of Mg-xCe-0.5Zn alloys by nano-indentation

K. C. PARK, B. H. KIM, Y. H. PARK, I. M. PARK

Department of Material Science and Engineering, Pusan National University,  
San 30 Jangjeon-dong, Geumjeong-gu, Busan 609-735, Korea

Received 23 September 2009; accepted 30 January 2010

**Abstract:** The microstructure and mechanical properties of Mg-xCe-0.5Zn ( $x=0.5, 1.5, 2.5$ , molar fraction, %) alloys were examined using a nano-indentation technique. The alloys were fabricated using a vacuum induction melting method under an argon atmosphere. The microstructures of Mg-xCe-0.5Zn alloys mainly consist of  $\alpha$ -Mg and eutectic Mg<sub>12</sub>Ce phase. The volume fraction and size of the eutectic Mg<sub>12</sub>Ce phase increase with increasing Ce contents. Nano-indentation test results show that the indentation hardness and elastic modulus of the eutectic Mg<sub>12</sub>Ce phase are higher than those of the  $\alpha$ -Mg matrix. In addition, the mean indentation hardness and elastic modulus of the Mg-xCe-0.5Zn alloys increase with the Ce addition amount increasing.

**Key words:** Mg alloys; Mg-Ce-Zn; rare earth; microstructure; mechanical properties; nano-indentation

### 1 Introduction

Mg alloys are widely used in structural parts, such as aerospace and automobile components, owing to their low density, excellent mechanical properties, superior electric shielding and superior damping capacity[1–4]. The addition of rare earth (RE) elements to Mg alloys has favorable effects on the high temperature mechanical properties. Therefore, to improve the mechanical and corrosion properties of Mg alloys containing RE elements, i.e. Ce, Y and Nd, has become an important issue. There have been many investigations[5–7] about the effect of RE addition on the microstructure and properties of Mg alloys. However, the influence of RE elements on the mechanical and corrosion properties of Mg alloys is not completely understood.

According to a Mg-Ce binary phase diagram [8], the maximum solubility of Ce in an  $\alpha$ -Mg matrix is 0.1% (molar fraction) at 590 °C and a Mg<sub>12</sub>Ce phase forms with up to 7.7% Ce (molar fraction) addition. However, the effect of Mg-Ce intermetallic compounds on the mechanical properties of Mg alloys is still unclear. It is reported that the addition of Zn improves the strength and ductility of Mg alloys through solid solution hardening. Considering the beneficial effects of Ce and

Zn addition in Mg alloys, therefore, it is very important to examine the microstructure and mechanical properties of Mg-Ce-Zn system. The aims of this study are to identify the phases and evaluate the mechanical properties of Mg-xCe-0.5Zn ( $x=0.5, 1.5$  and  $2.5$ ) (molar fraction, %) alloys by using a nano-indentation.

### 2 Experimental

Pure magnesium (99.8%), pure zinc (99%) and Mg-22%Ce (mass fraction) master alloy were used in this study. The alloys were fabricated using a vacuum induction melting method under an argon atmosphere. The nominal composition of the studied alloys was Mg-xCe-0.5Zn ( $x=0.5, 1.5, 2.5$ , molar fraction, %). For the microstructure observations, the samples were initially ground with emery paper and finally polished with 0.25  $\mu\text{m}$  diamond paste. The polished samples were etched with a 3% nital solution (97 mL ethanol and 3 mL nitric acid) for 3–5 s. The microstructure was examined with scanning electron microscope (SEM, Hitachi S-4300) equipped with an energy dispersive X-ray spectrometer (EDS). The phases were analyzed by X-ray diffractometry (XRD, Rigaku, CN2301) using monochromatic Cu K $\alpha$  radiation in the as-cast state. The volume fraction of the intermetallics was measured by

using an image analyzer.

Nano-indentation was performed using a Nanoindenter® XP (MTS) with a three-sided pyramidal diamond Berkovich indenter at a normal angle of  $65.3^\circ$  between the tip axis and the faces of the triangular pyramid, and a tip radius of approximately 20 nm. The indentation hardness and elastic modulus were obtained using the continuous stiffness measurement (CSM) technique. CSM is a powerful technique in providing information on mechanical properties such as hardness or elastic modulus of investigated materials. OLIVER and PHARR[9] reported a detailed description of the theory behind the CSM technique. Fig.1 shows the indentation positions required to measure hardness and modulus. A total of 8 indentations were made on each of the specimens and the penetration depths were approximately 500 nm. Each value of hardness and modulus was taken and averaged.

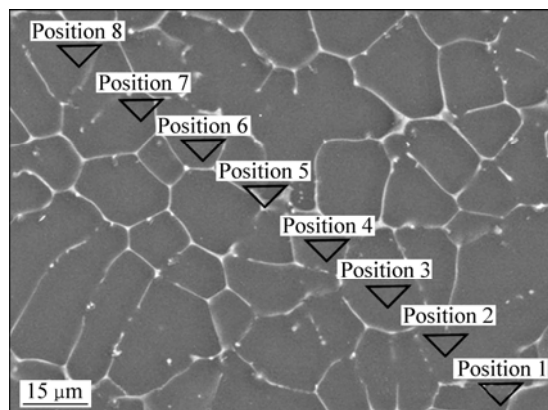


**Fig.1** Nano-indentation positions for measurement of hardness and modulus

### 3 Results and discussion

#### 3.1 Microstructure

Fig.2 shows the XRD patterns of the studied alloys. The alloys mainly consisted of  $\alpha$ -Mg and  $Mg_{12}Ce$  phases. On the other hand, neither the Ce-Zn intermetallic nor the ternary phase was detected. Fig.3 shows the SEM images of the experimental alloys. From the SEM-EDS results, the network phase was confirmed as  $Mg_{12}Ce$  phase and the isolated phase was confirmed as  $\alpha$ -Mg matrix. And as shown in Figs.3(a)–(c), these alloys exhibited a typical dendritic structure. When the Ce content was increased, the dendritic structures became more obvious and the dendrites were gradually refined. XIAO et al[10] reported that rare earth (RE) elements can refine the dendrite and grain size of Mg alloys. During solidification, rare-earth atoms concentrated at the solid/liquid interface due to their low solid solubility in  $\alpha$ -Mg. This enrichment prevented other solute atoms from diffusing to the solid phase, which results in the

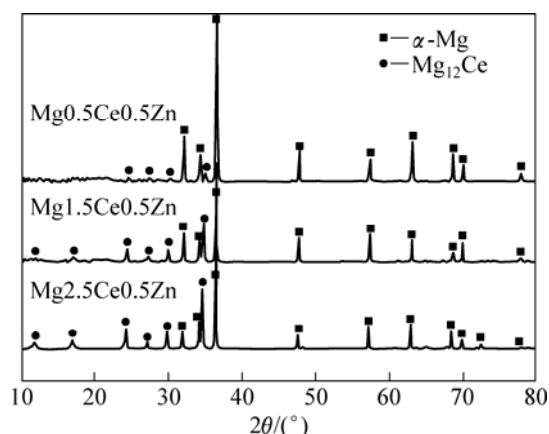


**Fig.2** XRD patterns of Mg-xCe-0.5Zn alloys

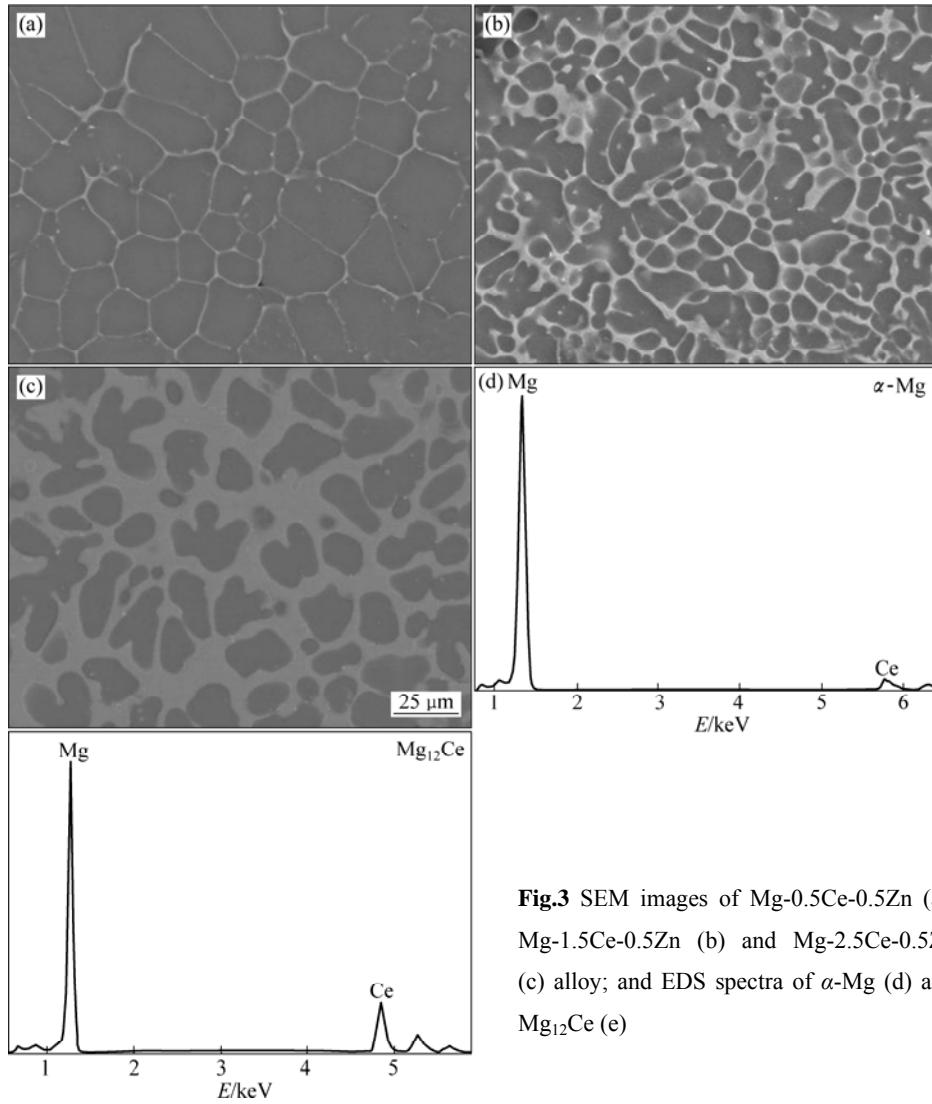
appearance of constitutional supercooling in front of the solid/liquid interface. Subsequently, the nucleation of the intermetallic phase was accelerated and these resulted in the restriction of dendrite growth.

Fig.4 presents the image analysis results for the volume fraction of the  $Mg_{12}Ce$  phase as a function of the Ce contents. The volume fraction of  $Mg_{12}Ce$  phase was increased with increasing the Ce contents and it was as high as about 42% with 2.5% Ce addition.

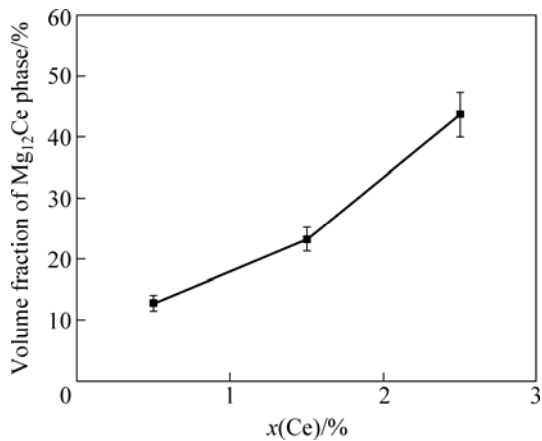
#### 3.2 Nano-indentation test

Fig.5 shows the load—displacement curves for both the eutectic  $Mg_{12}Ce$  phase and  $\alpha$ -Mg region of the  $Mg_{0.5}Ce_{0.5}Zn$  alloy. The shapes of the indentation load—displacement curves indicate the structural changes that occur within the indented material during the test. The loading curve of the eutectic region showed more fluctuations than that of the  $\alpha$ -Mg region. According to GE et al[11] and FENG and NGAN[12], the onset of dislocation slip, twinning and solid-phase transformation might be associated with discontinuities in the indentation load—displacement curves. For a given depth of 500 nm, the applied load for the  $Mg_{12}Ce$  phase was higher than that for the  $\alpha$ -Mg matrix. In Fig.5, the indentation hardness ( $H_{IT}$ ) of the  $Mg_{12}Ce$  phase and  $\alpha$ -Mg matrix was 1.4 and 1.0 GPa, respectively, and their elastic modulus ( $E$ ) was 51.2 and 44.3 GPa, respectively. The elastic recovery of the  $Mg_{12}Ce$  phase and  $\alpha$ -Mg region was approximately 13.1% and 10.2% of the maximum penetration depth, respectively.

Figs.6(a)–(c) show the indentation hardness and elastic modulus of the Mg-xCe-0.5Zn alloys according to the position. The indentation hardness and elastic modulus of the alloys had different values depending on the location where the indentation was taken. In addition, the mean indentation hardness and elastic modulus of alloys increased with increasing the concentration of the



**Fig.3** SEM images of Mg-0.5Ce-0.5Zn (a), Mg-1.5Ce-0.5Zn (b) and Mg-2.5Ce-0.5Zn (c) alloy; and EDS spectra of  $\alpha$ -Mg (d) and  $Mg_{12}Ce$  (e)



**Fig.4** Volume fraction of  $Mg_{12}Ce$  phase as function of Ce additions for Mg-Ce-Zn alloy

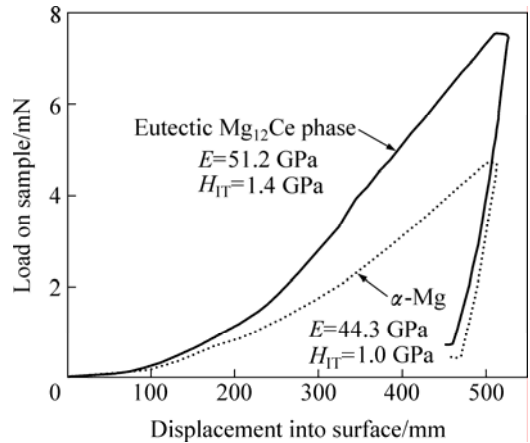


**Fig.5** Indentation load—displacement curves of both  $\alpha$ -Mg and eutectic regions of Mg-0.5Ce-0.5Zn alloy

$Mg_{12}Ce$  phase by Ce addition, as shown in Fig.6(d). It is postulated that the increased volume fraction of  $Mg_{12}Ce$  phase by Ce addition improved the mechanical

properties of Mg-Ce-Zn alloy. This means that Ce addition helps to increase the mechanical properties of Mg alloys.

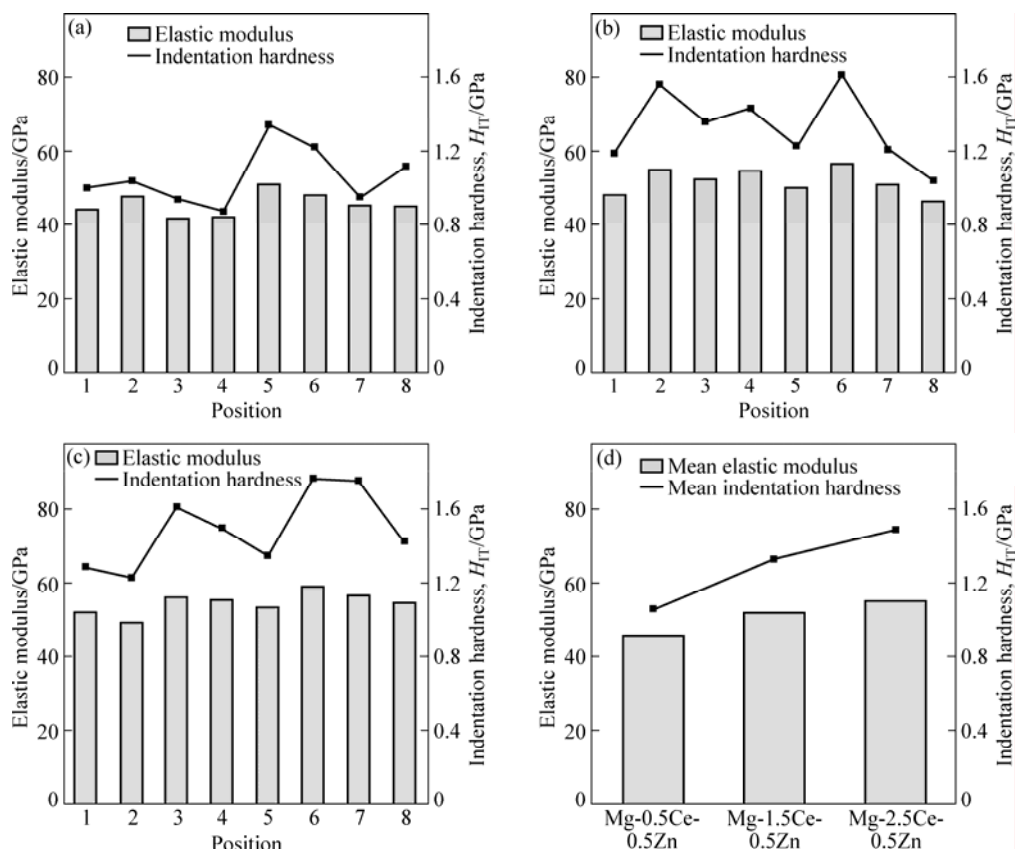


**Fig.6** Comparison of indentation hardness and modulus according to different positions: (a) Mg-0.5Ce-0.5Zn; (b) Mg-1.5Ce-0.5Zn; (c) Mg-2.5Ce-0.5Zn alloy; (d) Mean indentation hardness and elastic modulus

## 4 Conclusions

1) The microstructure of Mg-(0.5–2.5)Ce-0.5Zn (molar fraction, %) alloys consisted mainly of  $\alpha$ -Mg and eutectic Mg<sub>12</sub>Ce phases. The volume fraction of eutectic Mg<sub>12</sub>Ce phase increased with increasing the Ce content.

2) The indentation hardness and elastic modulus of the Mg<sub>12</sub>Ce phase were higher than those of the  $\alpha$ -Mg matrix. The mean indentation hardness and elastic modulus of the Mg-(0.5–2.5)Ce-0.5Zn (molar fraction, %) alloys were increased by the addition of Ce.

## Acknowledgments

This work was supported by a grant-in-aid for the National Core Research Center Program (No. R15-2006-022-02001-0) and the Metals Bank project of the Korea Ministry of Knowledge Economy.

## References

- [1] MORDIKE B L, EBERT T. Magnesium: Properties—applications—potential [J]. *Materials Science and Engineering A*, 2001, 302: 37–45.
- [2] KIM B H, LEE S W, PARK Y H, PARK I M. The microstructure, tensile properties, and creep behavior of AZ91, AS52 and TAS652 alloy [J]. *Journal of Alloys and Compounds*, 2010, 493: 502–506.
- [3] PARK K C, KIM B H, KIMURA H, PARK Y H, PARK I M.

Microstructure and corrosion properties of Mg-xSn-5Al-1Zn (x=0, 1, 5 and 9 mass%) alloys [J]. *Materials Transaction*, 2010, 51(3): 472–476.

- [4] PARK K C, KIM B H, JEON J J, PARK B G, PARK Y H, PARK I M. Influence of Sr and Zn additions on corrosion behaviour of Mg-6Sn-5Al-2Si alloys [J]. *International Journal of Cast Metals Research*, 2008, 21(1/3): 96–99.
- [5] BETTLES C J, GIBSON M A, ZHUC M A. Microstructure and mechanical behaviour of an elevated temperature Mg-rare earth based alloy [J]. *Materials Science and Engineering A*, 2009, 505: 6–12.
- [6] CHIA T L, EASTON M A, ZHU S M, GIBSON M A, BIRBILIS N, NIE J F. The effect of alloy composition on the microstructure and tensile properties of binary Mg-rare earth alloys [J]. *Intermetallics*, 2009, 17(7): 481–490.
- [7] WU An-ru, XIA Chang-qing. Study of the microstructure and mechanical properties of Mg-rare earth alloys [J]. *Materials & Design*, 2007, 28(6): 1963–1967.
- [8] MASSALSKI T B. Binary alloy phase diagrams [M]. 2nd ed. Materials Park, Ohio: ASM International, 1990.
- [9] OLIVER W C, PHARR G M. An improved technique for determining hardness and elastic modulus using load and displacement sensing indentation experiments [J]. *Journal of Materials Research Society*, 1992, 7: 1564–1583.
- [10] XIAO W, JIA S, WANG J, YANG J, WANG L. The influence of mischmetal and tin on the microstructure and mechanical properties of Mg-6Zn-5Al-based alloys [J]. *Acta Materialia*, 2008, 56: 934–941.
- [11] GE D, DOMNICH V, JULIANO T, STACH E A, GOGOTSI Y. Structural damage in boron carbide under contact loading [J]. *Acta Materialia*, 2004, 52: 3921–3927.
- [12] FENG G, NGAN A H W. Creep and strain burst in indium and aluminium during nanoindentation [J]. *Scripta Materialia*, 2001, 45: 971–976.

(Edited by YANG Bing)